Polymer Chemistry

Accepted Manuscript

This is an *Accepted Manuscript*, which has been through the Royal Society of Chemistry peer review process and has been accepted for publication.

Accepted Manuscripts are published online shortly after acceptance, before technical editing, formatting and proof reading. Using this free service, authors can make their results available to the community, in citable form, before we publish the edited article. We will replace this *Accepted Manuscript* with the edited and formatted *Advance Article* as soon as it is available.

You can find more information about *Accepted Manuscripts* in the Information for Authors.

Please note that technical editing may introduce minor changes to the text and/or graphics, which may alter content. The journal's standard Terms & Conditions and the Ethical guidelines still apply. In no event shall the Royal Society of Chemistry be held responsible for any errors or omissions in this *Accepted Manuscript* or any consequences arising from the use of any information it contains.

ROYAL SOCIETY OF CHEMISTRY

www.rsc.org/polymers

Cite this: DOI: 10.1039/c0xx00000x

www.rsc.org/xxxxxx

ARTICLE TYPE

Functional porous membranes from amorphous linear dendritic polyester hybrids

Surinthra Mongkhontreerat,[a] Marie V. Walter,[a] Yanling Cai,[a] Hjalmar Brismar,[b] Anders Hult,[a] and Michael Malkoch*[a]

Received (in XXX, XXX) Xth XXXXXXXXX 20XX, Accepted Xth XXXXXXXXX 20XX
DOI: 10.1039/b000000x

By combining ATRP, dendrimer chemistry and 'click' reactions, a library of novel linear dendritic block copolymers (hybrids) was successfully synthesized. The isolated polymers displayed hydrophilic alkyne groups and Tg's ranging from 14 °C to 67 °C. A Tg threshold of 39 °C was found necessary for straightforward porous membrane fabrication via Breath Figure method. Exploiting the copper(I)-catalyzed azide-alkyne cycloaddition (CuAAC) reaction, a robust and benign protocol was identified enabling surface functionalizations in aqueous conditions. Such manipulations included the introduction of fluorescent rhodamine for thorough assessment by confocal fluorescent microscopy as well as polyethylene glycol chains or perfluorinated groups for tuning the membrane wettability. Finally, with the initial indication of being nontoxic to human dermal fibroblasts (hDF) and osteoblast-like MG63, the porous membranes can potentially find use in the field of controlled cell culture such as patterning of cell growth.

Topological alternation of a surface, from flat to porous, increases the surface area which dramatically changes the substrate properties. Such manipulation substantially broadens the performance window of a desired substrate and therefore porous surfaces are found in a range of applications from biosensors, protein patterning,[1,2] templates for soft lithography[3] and electronics.[4] Today, the Breath Figure (BF) method, introduced in the late 1990's by François *et al*.,[5,6] is recognized as a facile, robust and low cost route to generate porous polymeric films on solid substrates. It capitalizes on drop casting hydrophobic polymers from volatile organic solvents on inorganic substrates under humid conditions in which water droplets act as a porous template. Polymer architectures, solvent polarities and rate of evaporation are examples of parameters of great importance for porous film formation, which need to be tuned for each system. From the great number of honeycomb surfaces achieved, polystyrene architectures including linear, star shaped polymer and copolymer with polyparaphenylene and poly 3- hexylthiophene[6] have successfully generated ordered honeycomb films. Furthermore, the effect of polystyrene chain-ends on formation of isoporous membranes was reported by Hawker and co-workers. The elegant work exploited polystyrene stars hybridized with dendron blocks of different sizes based on 2,2,-bis(methylol) propionic acid (bis-MPA).[7] Altering the size of the dendritic wedges and their peripheral functionalities radically changed the pore morphology, from closed sphere-liked pores to cylindrical open pores. For amphiphilic block copolymers, the characteristic mechanism for producing isoporous films is crucially coupled to adjusting the hydrophobic to hydrophilic ratio and therefore the interfacial tension. Amphiphilic block copolymers which comprise bis-MPA dendritic components are nowadays attractive candidates to fabricate passive drug delivery systems.[8,9] In the context of generating isoporous membranes, the influence of dendritic components using amphiphilic block copolymers from challenging semi-crystalline polycaprolactone (PCL) was elaborated by Malkoch *et. al*.[10,11] By utilizing dendrons as dendritic linkers, a library of amphiphilic block copolymer hybrids was synthesized based on hydrophilic polyethylene glycol (PEG) segments and hydrophobic PCL components. In the study, the addition of dendritic wedges resulted in increased stabilization of water droplets, which lead to more ordered isoporous film formation. The most profound effect on pore ordering was found when a single 2 kDa PEG and eight PCL chains where interconnected via a third generation dendron, ($PEG2kG3(PCL30)_8$). The increased ordering was proposed to be an effect of the dendritic linker resulting in lower density hybrid polymers, due to the introduced branches along with increased interfacial tension. Even though dendritic wedges have shown positive impact as promoters of honeycomb membranes, their scaffolding ability to generate functional surfaces via facile postfunctionalization strategies is still lacking. With the increasing need of substrates displaying diverse surface functionalities, we herein propose a novel family of amorphous linear dendritic hybrids that deliver functional porous membranes where both the linear and dendritic blocks consist of bis-MPA as a key building block.

The sought out hybrids were designed to comprise linear hydrophobic components that enable formation of stable films and dendritic wedges with dual function, being both hydrophilic to stabilize the water droplets as well as reactive to straightforwardly introduce desired surface functionalities. 2-Hydroxyethyl methacrylate (HEMA) (**1**) was reacted with activated benzylidene-protected bis-MPA (**2**) using traditional anhydride chemistry resulting in benzylidene functional HEMA monomer, HEMA-Bz **(3)**, in 98% isolated yield, Scheme 1. The benzylidene group was selected to introduce bulkiness and

Polymer Chemistry Accepted Manuscript

Cite this: DOI: 10.1039/c0xx00000x

www.rsc.org/xxxxxx

ARTICLE TYPE

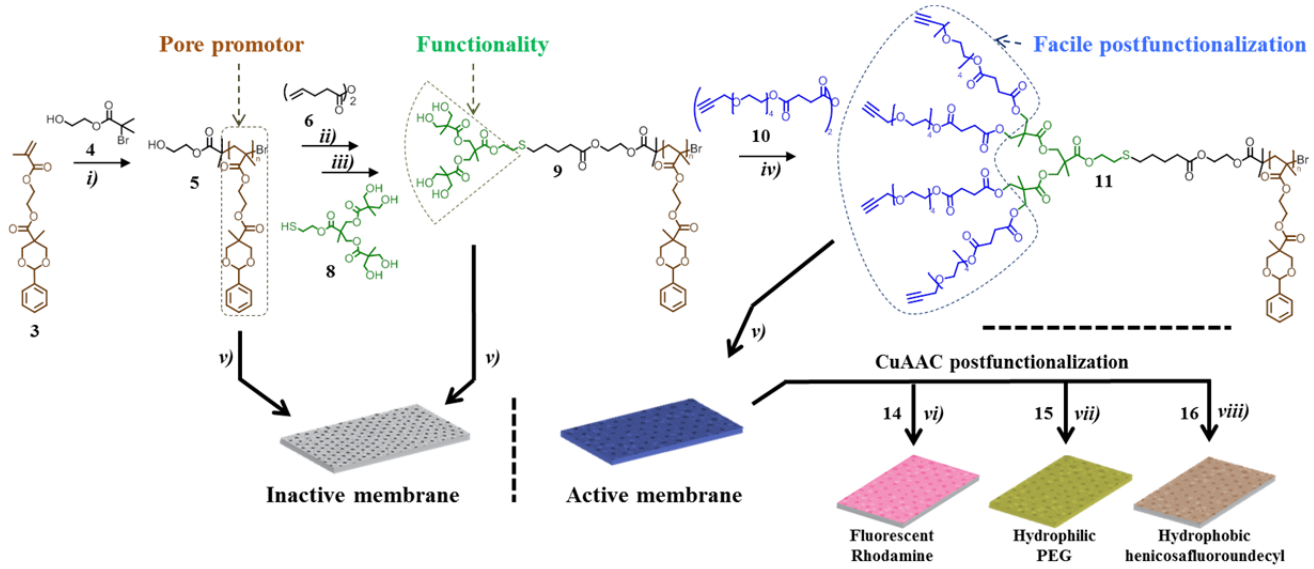

Scheme 1 Overall strategy including: i)-iv) synthesis of linear dendritic hybrid library; v) formation of porous film via breath figure method; and aqueous CuAAC functionalization of surfaces with azide functional vi) Rhodamine dye, vi) PEG, and viii) henicosafluoroundecyl.

hydrophobic properties to the polymer chains along with anticipated increased Tg required to generate stable porous films at room temperatures. The monomer (**3**) was polymerized using standard Atom Transfer Radical Polymerization (ATRP) conditions from 2-hydroxyethyl 2-bromoisobutyrate (**4**) as an initiator.[12] The targeted degree of polymerization (DP_{target}) was set to 15 or 65 at 50% conversion corresponding to molecular weights of 5 000 and 22 000 $gmol^{-1}$ respectively (referred to as **P5** and **P22**). As seen in Table 1, the dispersity (Đm) calculated by SEC for the linear polymers **P5** and **P22** were 1.16 and 1.08, respectively. The obtained SEC molecular weight of **P5** was found to be close to the targeted value i.e. ca 4 500 $g.mol^{-1}$ whilst **P22** revealed a lower molecular weight of 12 900 $g.mol^{-1}$. End-group integrations of **P5** and **P22** by ^{1}H-NMR yielded molecular weights of 5 700 $g.mol^{-1}$ and 10 000 $g.mol^{-1}$, respectively. Consequently, the molecular weight discrepancy of **P22** is due to the fact that the monomer conversion only reached 36%.

To extend the hydrophobic polymers with hydrophilic and functional blocks, bis-MPA based dendrons of generation (G) one (**13**) and two (**8**) with a single thiol at the focal point were chosen.[13] Prior to hybridization via UV initiated thiol-ene coupling chemistry (TEC),[11,14,15] **P5** and **P22** chain-ends were allyl functionalized with 4-pentanoic anhydride (**6**), Scheme 1 and Table 1. For direct comparison, covalent attachment of mercaptoethanol (**12**) was also sought out as a linear analogue (G0). All hybridization reactions were successfully accomplished in DCM for 30 min at 365 nm. It should be noted that an increase in Đm was obtained for the hybridization of **P22** systems which may be an effect of more complex conformations obtained when eluting in DMF. Further modifications of the hydroxyl groups was achieved by the reaction with bifunctional alkyne-tetraethylene glycol anhydride (**10**) (TEG-Alk), Figure S1. ^{1}H-NMR confirmed the success of all reaction steps i.e. allylation (*ii*), TEC (*iii*) and final modification with acetylene groups (*iv*). The dendritic components offer accurate access to more chain-end groups, whilst the TEG-Alk provides both increased hydrophilicity and postfunctionalizable groups available for subsequent CuAAC 'click' reaction in aqueous conditions.

As can be seen in Table 1, the introduction of dendron wedges decreases the glass transition temperatures. This can be due to the dendritic wedges decreasing the entanglement of polymer chains and therefore increasing chain mobility.[16,17] For instance, after the attachment of G2-TEG-Alk to **P5** and **P22** with Tg of 65 and 67 °C, the resulting block copolymers **P5-5** and **P22-5** exhibit a Tg decrease to values of 14 and 39 °C, respectively.

Satisfied with the isolated library of highly sophisticated linear dendritic hybrids, the fabrication of porous films was assessed through BF method. After condition optimizations, porous films were generated on glass substrates from chloroform with 40μL of 20 $g.L^{-1}$ polymer concentration at 90% relative humidity and room temperature. Table S1 illustrates Scanning Electron Micrographs (SEM) of porous surfaces obtained from the hybrid library. All polymers resulted in porous films with pore sizes ranging from 0.26 to 1.6 μM except Alk-TEG modified 5k polymers **P5-3**, **P5-4** and **P5-5**. The inability to form porous films from 5k systems with ca 15 repeating unit is evidently affected by the hydrophilic nature of Alk-TEG disturbing the stabilization of water droplets. An additional destabilizing effect is correlated to the low Tg obtained for these polymers, ranging from 14 to 32 °C, resulting in more mobile solid films. As demonstrated in Figure 1a, at a Tg of 39 °C and above, stable porous films were

Polymer Chemistry Accepted Manuscript

accomplished for these systems under typical BF processes using $CHCl_3$ as volatile solvent.

Table 1 Characterization of linear dendritic hybrids

Linear segment	Dendritic wedge	Polymer code	$M_{n,theo}$ [a] [g.mol^{-1}]	$M_{n,SEC}$ [b] [g.mol^{-1}]	Dispersity [b] ($Đ_m$)	T_g [c] [°C]
Poly(HEMA-Bz)-5k	OH	P5	5 200	4 500	1.16	65
	G0-OH	P5-0	5 300	4 900	1.10	47
	G1-OH	P5-1	5 500	6 100	1.24	48
	G2-OH	P5-2	5 700	6 700	1.06	52
	G0-TEG-Alk	P5-3	5 700	5 800	1.07	32
	G1-TEG-Alk	P5-4	6 100	6 800	1.05	27
	G2-TEG-Alk	P5-5	6 100	7 800	1.04	14
Poly(HEMA-Bz)-22k	OH	P22	22 000	12 900	1.08	67
	G0-OH	P22-0	22 200	16 100	1.56	62
	G1-OH	P22-1	22 300	14 400	1.41	58
	G2-OH	P22-2	22 500	16 900	1.57	54
	G0-TEG-Alk	P22-3	22 500	16 100	1.53	39
	G1-TEG-Alk	P22-4	22 900	14 800	1.45	47
	G2-TEG-Alk	P22-5	22 800	14 600	1.48	39
	G2-TEG-Rh	P22-6	26 000	15 000	1.21	62

[a]Calculated assuming 50% conversion. [b] Determined from DMF SEC, [c] Obtained from DSC

From the number of fabricated porous films the hybrid **P22-5** was selected for a comprehensive property assessment as it comprises a large hydrophobic block as well as displaying a G2 hydrophilic dendron with highest functionality per chain. The top view of **P22-5** porous membrane shown in Fig. 1b) and c) details pores of different sizes ranging from 0.016 μm^2 to 1.76 μm^2 with an average pore size of 0.43 $\mu m^2 \pm 0.47$. Interestingly, after peeling the top layer with an adhesive tape, the underlying layer revealed more ordered porous structures, Fig. 1d. The cross section revealed dual-layer interconnected porosity, Fig. 1e, generated from diffused water droplets in the organic solution. Compared to a flat surface, the generated porosity increases the surface area by 250%, calculated from SEM with imageJ software (see Table S1 and Fig S3). As the morphology of films are greatly influenced by the casting conditions, the alternation from standard casting condition (20 mg.mL^{-1}, RT) to more diluted (2.5 mg.mL^{-1}, at 0 °C) resulted in a membrane with open structure for **P22-5** with average pore size of 2.6 $\mu m^2 \pm 0.64$, Fig. 1f. At a lower polymer concentration, a lower evaporation rate (i.e. lower temperature) of the chloroform is required to stabilize the pore formation. The polymer concentration of 2.5 mg.mL^{-1} is not sufficient to fully cover the water droplets and results in a film with a more open structure. For the exploitation in biological applications, the critical requirement for any porous substrate is that it needs to sustain physiological conditions including pH and temperatures. In this context, porous membranes from **P22-5** were soaked in buffer solutions of citric acid and Na_2HPO_4 with pH ranging from 4-8 for 30 minutes. Notably, the films were found stable considering that the hydrophobic polymer block contains a large number of acid labile benzylidene groups, Table S2. In terms of thermal stability, the membranes endured temperature above the Tg of 39 °C for **P22-5** prior to collapse at 50 °C as shown in Table S3.

Modular and facile functionalization protocols of flat or porous substrates are vital to introduce desired function and secure specific end-properties. In contrast to the inactive surfaces based on OH-functional block copolymers, the presence of hydrophilic blocks with accessible alkyne groups within the hybrids were

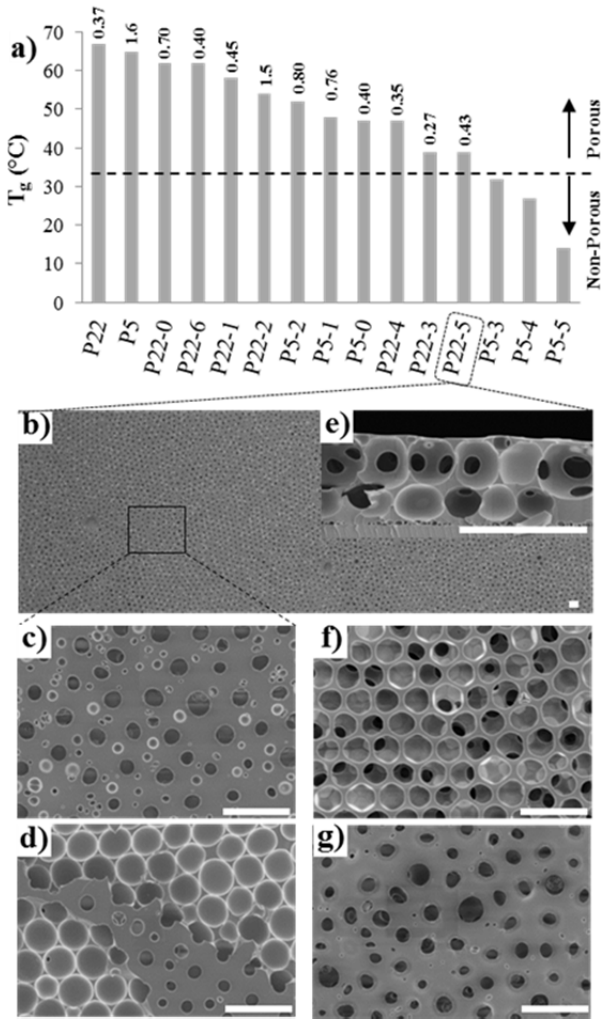

Fig. 1 a) glass transition temperature of the library of linear dendritic hybrid where the dash line shows the critical lowest Tg below which the porous film could not be formed, b) to g) SEM images of P22-5 porous films (5 µm scale bar): b) large area of top view, c) closed pores structure, d) ordered structure after the top layer was peeled of, e) cross section of the film, f) open pored structure when casting from 2.5 mg.ml-1 solution at 0 °C and g) stable porous film after postfunctionalization via CuAAc in water.

envisioned to allow a simple yet efficient surface functionalization strategy of surfaces. By exploiting the robustness of CuAAC chemistry in aqueous conditions, straightforward postfunctionalizations were anticipated without disrupting the porous features of already generated films. Consequently, porous film based on **P22-5** was submerged in deionized water containing azide functional rhodamine B **(14)** fluorescent dye, sodium ascorbate and $CuSO_4$. The reaction was allowed to proceed for 30 min and thereafter terminated by washing cycles with deionized water. As can be seen in Fig 1g, the integrity of the porous structure was still maintained after postfunctionalization. Confocal fluorescence microscopy was utilized to evaluate the attachment profile of the dye, Fig. 2a.

The fluorescence signal was visualized in white on the micrographs while the depth profile represents the emission signal at different depths under the film. The micrographs clearly show the diffusion of the dye into the porous membrane and

Polymer Chemistry Accepted Manuscript

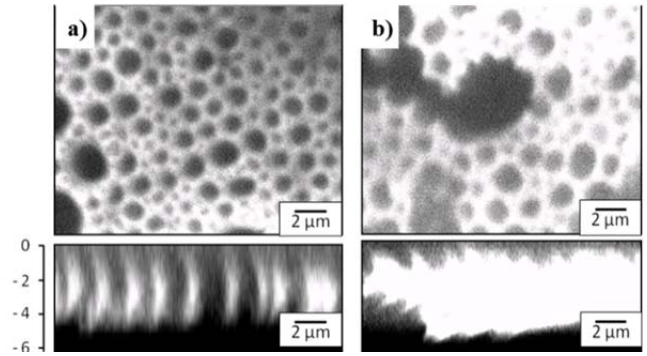

Fig. 2 Confocal fluorescence microscopy and depth profile in Y axis of a) closed pore structure of P22-5 after surface postfunctionalization with rhodamine-N3 and b) P22-6

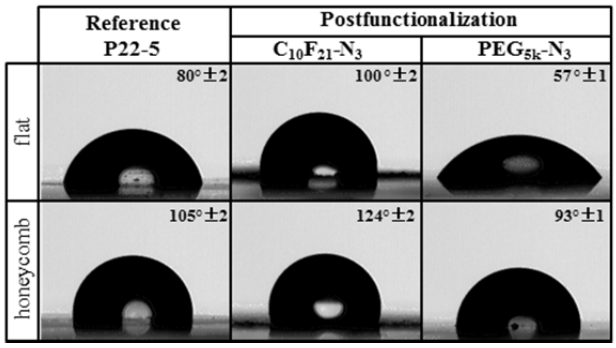

Fig. 3 Contact angle measurement of flat and porous surface of P22-5 before and after modification with hydrophilic PEG 5k and hydrophobic henicosafluoroundecyl moities via CuAAC chemistry.

successful topological attachment to the surface. As a comparison, a rhodamine functionalized hybrid **P22-6** was synthesized and porous films were generated under similar conditions as stated earlier. The fluorescence signal for the **P22-6** can be detected throughout the membrane as seen in Fig. 2b. The porous films obtained from **P22-6** suggest further optimization is necessary to generate more regular porous films.

Based on these results, it is apparent that the postfunctionalization strategy of premade regular porous substrates is intrinsically more robust and modular. To further corroborate on the facile surface manipulations, azide functional hydrophilic 5k PEG **(16)** and hydrophobic henicosafluoroundecyl 6-azidohexanoate **(15)** were reacted with **P22-5** films to alter the wettability of the membranes. In one case, for application where porous membranes are used as templates for replicating, the surfaces should be hydrophobic for easy release from the replica.[4] In another case, for micro container-type applications[18] where the pores can be used for study of DNA or polymer infiltration, the surfaces need to be hydrophilic to enable the solution to penetrate into the pore and overcome the capillary effect of microstructures. Subsequently, both porous and flat substrates were postfunctionalized and contact angles (CA) were measured, Fig 3. In all cases, the porous membranes were intact and displayed higher contact angles compared to flat surfaces. This phenomena is related to the increased surface roughness of the substrate.[19] The CuAAC reaction with henicosafluoroundecyl group required the use of methanol as a co-solvent and resulted in surfaces with a CA of 100° for flat and 124° for the porous structure. On the other hand, for the surface functionalization with PEG-N_3, the contact angle decreased from 80° to 57° for the flat surface and 105° to 93° for the porous film.

Considering the potential use in biological applications, the cytotoxicity profile of **P22-5** was evaluated through both elution test according to ISO 10993-5 procedures[20] as well as direct cell growth.[21-25] No cytotoxicity was observed for the polymer in the tests with two human cell lines, human dermal fibroblasts (hDF) and osteoblast-like MG63 (See Fig. S4). The influence of porous and flat surfaces on cell adhesion was assessed using hDF cell line. As illustrated in Fig 4, the cells are prone to grow on the flat surface rather than the porous counterpart. These findings contradict earlier findings and thus highlights the complexity of cell growth, which is influenced by type of cell as well as the micro environment[26] such as modulus,[27] surface structure,[21,28] wettability[22] and functionalities.[23,29] Earlier reports conclude that structured surfaces enhance cell adhesion; however, the systems assessed possessed higher hydrophilicity.[22,25,30] A possible explanation could be that the flat film of **P22-5** with a CA of 80° is defined as hydrophilic whilst the porous substrate having a CA of 105° is considered hydrophobic. Independently, due to the facile fabrication method, these structured membranes can potentially be used to manipulate cell patterning[26] where controlled growth location is important.

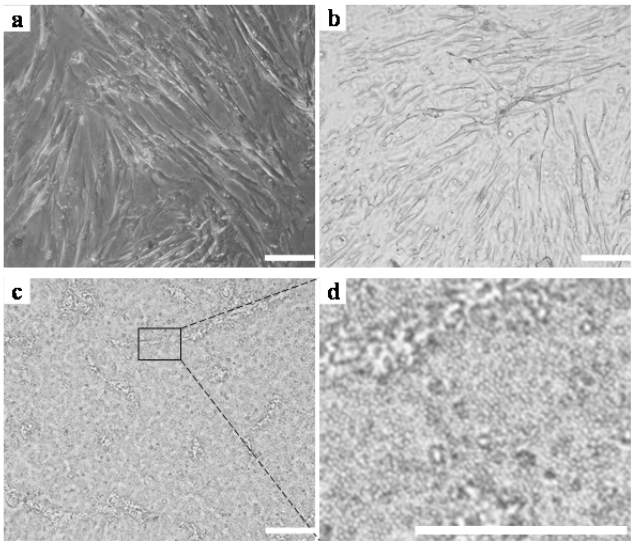

Fig. 4 Growth of hDF on a) controlled plate, b) flat film of P22-5, c) porous P22-5 film and d) zoom in of c) showing the deformation of porous film, not the attachment of the cell (scale bar represents 100 µm)

In conclusion, a library of novel linear dendritic polyester hybrids based on bis-MPA was successfully synthesized possessing reactive alkynes. By utilizing the BF method, porous membranes were successfully fabricated and straightforwardly postfunctionalized under benign aqueous conditions with hydrophilic PEG, hydrophobic henicosafluoroundecyl and rhodamine dye using CuAAC 'click' chemistry. With the initial indication of being non-toxic along with the absence of cell adhesion, these porous films could find potential use in cell growth patterning.

We acknowledge AB WILH. BECKERS Jubileumsfond and Swedish Research Council (grants 2011-4477 and 2010-453) for financial support. Swedish SciLifeLab biomaterial platform is

Polymer Chemistry Accepted Manuscript

This journal is © The Royal Society of Chemistry [year]

acknowledged for the cell study setup.

Notes and references

[a] KTH Royal Institute of Technology, School of Chemical Science and Engineering, Dept. of Fibre and Polymer Technology, SE-100 44, Stockholm, Sweden. Tel: +46 8790 8768; E-mail: malkoch@kth.se
[b] KTH Royal Institute of Technology, Science for Life Laboratory, School of Engineering Sciences, Division of Cell Physics,SE-106 91 Stockholm, Sweden

† Electronic Supplementary Information (ESI) available: See DOI: 10.1039/b000000x/

(1) Min, E.; Wong, K. H.; Stenzel, M. H. *Adv. Mater. (Weinheim, Ger.)* **2008**, *20*, 3550.
(2) Zhang, Y.; Wang, C. *Adv. Mater. (Weinheim, Ger.)* **2007**, *19*, 913.
(3) Vohra, V.; Yunus, S.; Attout, A.; Giovanella, U.; Scavia, G.; Tubino, R.; Botta, C.; Bolognesi, A. *Soft Matter* **2009**, *5*, 1656.
(4) Pintani, M.; Huang, J.; Ramon, M. C.; Bradley, D. D. C. *J Phys-Condens Mat* **2007**, *19*.
(5) Widawski, G.; Rawiso, M.; Francois, B. *Nature* **1994**, *369*, 387.
(6) François, B.; Pitois, O.; François, J. *Advanced Materials* **1995**, *7*, 1041.
(7) Connal, L. A.; Vestberg, R.; Hawker, C. J.; Qiao, G. G. *Advanced Functional Materials* **2008**, *18*, 3706.
(8) Pahovnik, D.; Čusak, A.; Reven, S.; Žagar, E. *Journal of Polymer Science Part A: Polymer Chemistry* **2014**, *52*, 3292.
(9) Hed, Y.; Zhang, Y.; Andrén, O. C. J.; Zeng, X.; Nyström, A. M.; Malkoch, M. *Journal of Polymer Science Part A: Polymer Chemistry* **2013**, *51*, 3992.
(10) Lundberg, P.; Walter, M. V.; Montanez, M. I.; Hult, D.; Hult, A.; Nystrom, A.; Malkoch, M. *Polymer Chemistry* **2011**, *2*, 394.
(11) Walter, M. V.; Lundberg, P.; Hult, D.; Hult, A.; Malkoch, M. *Polymer Chemistry* **2013**, *4*, 2680.
(12) Matyjaszewski, K. *Macromolecules* **2012**, *45*, 4015.
(13) Feliu, N.; Walter, M. V.; Montanez, M. I.; Kunzmann, A.; Hult, A.; Nystrom, A.; Malkoch, M.; Fadeel, B. *Biomaterials* **2012**, *33*, 1970.
(14) Walter, M. V.; Lundberg, P.; Hult, A.; Malkoch, M. *J Polym Sci Pol Chem* **2011**, *49*, 2990.
(15) Ghirardello, M.; Öberg, K.; Staderini, S.; Renaudet, O.; Berthet, N.; Dumy, P.; Hed, Y.; Marra, A.; Malkoch, M.; Dondoni, A. *Journal of Polymer Science Part A: Polymer Chemistry* **2014**, *52*, 2422.
(16) Andrén, O. C. J.; Walter, M. V.; Yang, T.; Hult, A.; Malkoch, M. *Macromolecules* **2013**, *46*, 3726.
(17) Carlmark, A.; Malmstrom, E.; Malkoch, M. *Chem Soc Rev* **2013**, *42*, 5858.
(18) Bunz, U. H. F. *Advanced Materials* **2006**, *18*, 973.
(19) Gao, L.; McCarthy, T. J.; Zhang, X. *Langmuir* **2009**, *25*, 14100.
(20) *ISO 10993-5: Biological evaluation of medical devices - Part 5: Tests for in vitro cytotoxicity* **2009**.
(21) Nishikawa, T.; Nonomura, M.; Arai, K.; Hayashi, J.; Sawadaishi, T.; Nishiura, Y.; Hara, M.; Shimomura, M. *Langmuir* **2003**, *19*, 6193.
(22) Li, L.; Chen, C.; Li, J.; Zhang, A.; Liu, X.; Xu, B.; Gao, S.; Jin, G.; Ma, Z. *Journal of Materials Chemistry* **2009**, *19*, 2789.
(23) Du, M.; Zhu, P.; Yan, X.; Su, Y.; Song, W.; Li, J. *Chemistry – A European Journal* **2011**, *17*, 4238.
(24) Hernandez-Guerrero, M.; Stenzel, M. H. *Polymer Chemistry* **2012**, 3, 563.
(25) Beattie, D.; Wong, K. H.; Williams, C.; Poole-Warren, L. A.; Davis, T. P.; Barner-Kowollik, C.; Stenzel, M. H. Biomacromolecules 2006, 7, 1072.
(26) Guillotin, B.; Guillemot, F. Trends in Biotechnology 2011, 29, 183.
(27) Engler, A. J.; Sen, S.; Sweeney, H. L.; Discher, D. E. Cell 2006, 126, 677.
(28) Itoh, H.; Aso, Y.; Furuse, M.; Noishiki, Y.; Miyata, T. Artificial Organs 2001, 25, 213.
(29) Wischerhoff, E.; Uhlig, K.; Lankenau, A.; Börner, H. G.; Laschewsky, A.; Duschl, C.; Lutz, J.-F. Angewandte Chemie International Edition 2008, 47, 5666.
(30) Barbetta, A.; Dentini, M.; De Vecchis, M. S.; Filippini, P.; Formisano, G.; Caiazza, S. Advanced Functional Materials 2005, 15, 118.

Polymer Chemistry Accepted Manuscript